Photoinduced Cooperative Reorientation in Photoreactive Hydrogen-Bonded Copolymer Films and LC Alignment Using the Resultant Films

Nobuhiro Kawatsuki,* Takayuki Kawanishi, and Emi Uchida

Department of Materials Science and Chemistry, Himeji Institute of Technology, University of Hyogo, 2167 Shosha Himeji, 671-2280 Japan

Received March 6, 2008; Revised Manuscript Received May 6, 2008

ABSTRACT: Polymethacrylate copolymers, which have hexamethylene spacer groups terminated with 4-oxycinnamic acid, 4-oxybenzoic acid, and 4-(4′-oxyphenyl)benzoic acid in the side chain, were synthesized, and the photoinduced cooperative molecular reorientation of thin films was demonstrated using linearly polarized ultraviolet (LPUV) light and subsequent annealing. Adjusting the exposure doses can control the molecular reorientation direction both perpendicular and parallel to the polarization **E** of LPUV light. Tuning the copolymer composition adjusted the optical birefringence of homogeneously reoriented films between 0.095 and 0.178. Finally, adjusting the exposure doses achieved uniform alignment control of low-molecular liquid crystals (LCs) on the molecular reoriented copolymer films both perpendicular and parallel to the polarization **E** of LPUV light.

1. Introduction

The photoinduced orientation of polymeric films has received much attention due to its potential capability as many kinds of optical and photonics applications. Numerous studies have reported an axis-selective *trans*−*cis*−*trans* photoisomerization in azobenzene molecules[1,2,4–10] and photo-cross-linkable polymeric materials[11–16] to generate the photoinduced optical anisotropy. Among them, polymeric films comprised of cinnamate or coumarin derivatives are transparent in the visible region, and are axis-selectively photoreacted by irradiating with LP ultraviolet (LPUV) light.[11,12] For example, a polyvinyl cinnamate (PVCi) film exhibits a small photoinduced optical anisotropy after irradiating with LPUV light, and the resultant film is applicable to the photoalignment layer for low-molecular liquid crystalline (LC) molecules.[13–16] To generate a large optical anisotropy, a molecular reorientation should accompany the axis-selective photoreaction. For the photoreactive materials attaining a large molecular reorientation, we carried out a systematic study on photo-cross-linkable liquid crystalline polymers (PLCPs) terminated with cinnamate derivatives.[5,17–21] Irradiating the PLCP films with LPUV light generates a photoinduced optical anisotropy, and a subsequent thermal treatment enhances the molecular reorientation due to the LC characteristics of the material. The transparent reoriented films are applicable to passive optical devices such as birefringent films,[22] the LC alignment layers for liquid crystal displays,[16,23] and polarization holographic gratings.[24] Among them, we have reported that a polymethacrylate comprised of a hexamethylene spacer group terminated with a 4-oxycinnamic acid (CA) in its side chain (**P6CA**) exhibits a large photoinduced molecular reorientation with a high photoreactivity toward LPUV light.[21] Due to the hydrogen(H)-bonded dimers of the 4-oxycinnamic acid moieties, **P6CA** exhibits a LC mesomorphism similar to polymers terminated with 4-oxybenzoic acid (BA) in their side chains.[25–30] An axis-selective photoreaction of the 4-oxycinnamic acid groups of the **P6CA** film induces a small optical anisotropy, and the subsequent annealing process thermally generates the self-organization of the mesogenic groups.[21] Furthermore, adjusting the exposure doses achieves uniform alignment control of low-molecular LCs on the resultant film, but a detailed investigation of the LC alignment behavior has yet to be explored.

Cooperative photoinduced molecular reorientation is often observed in azobenzene-containing polymers and PLCPs copolymerized with comonomers comprised of nonphotoreactive mesogenic side groups.[31–38] The functionality of the reoriented films may be derived from cooperative reorientation, while the controllability of the molecular reorientation behavior may be due to tuning of the comonomer. Several LC copolymers, which containing H-bonded mesogenic side groups, have been explored.[39–43] Lin et al. have synthesized and characterized H-bonded copolymers with BA groups and stilbazole side groups.[39] Gao et al. have investigated the surface relief formation in an azobenzene-containing supramolecular polymer film.[40] Medvedev et al. have reported the laser-induced molecular reorientation behavior of methacrylate copolymer films with 4-cyanobiphenyl and BA side groups doped with azobenzene monomer stabilized by H-bonds.[41] In addition, we have studied methacrylate copolymer films with photoreactive 4-(4-methoxycinnamoyloxy)biphenyl (MCB) and BA groups in their side chains, and found that they exhibit a thermally enhanced cooperative molecular reorientation when the composition of the MCB side groups is less than 50 mol %.[43] With a higher content of MCB groups, molecular reorientation is not observed due to the decomposition of the H-bonds of the BA moieties, although the copolymer shows a LC mesophase at all the copolymer compositions. These observations suggest that the H-bonded aromatic dimeric structure is important for the cooperative molecular reorientation for the PLCPs containing H-bonded mesogenic side groups. When copolymers contain different aromatic acid groups in their side chains, aromatic acids will randomly form the H-bonded LC dimers, which show different optical and thermal properties from the homopolymer. However, copolymers with a spacer group terminated with CA and nonphotoreactive aromatic acid groups as well as their photoinduced reorientation behavior have yet to be examined.

In these contexts, one purpose of this paper is to synthesize new H-bonded photo-cross-linkable LC copolymers comprised of photoreactive and nonphotoreactive aromatic acid side groups, which can control the photoinduced optical birefringence of the cooperatively reoriented copolymer films. New H-bonded methacrylate copolymers comprised of a hexamethylene spacer group terminated with CA side groups and BA or 4-oxyphenylbenzoic

* To whom correspondence should be addressed. E-mail: kawatuki@eng.u-hyogo.ac.jp. Telephone: +81-792-67-4886. Fax: +81-792-66-4885.

10.1021/ma800505c CCC: $40.75
Published on Web 06/11/2008

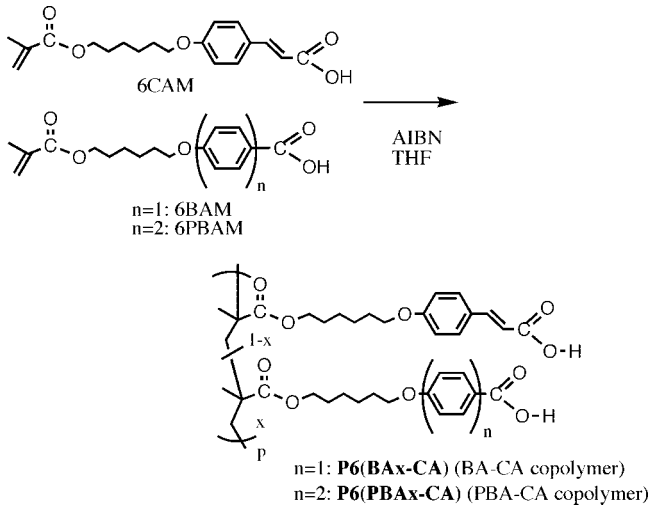

Figure 1. Synthetic route to copolymers used in this study.

acid (PBA) side groups (Figure 1) are synthesized, and their thermally enhanced photoinduced molecular reorientation and the influence of the nonphotoreactive acid groups on the reorientation behavior are investigated. Because all the aromatic acid groups form H-bonded mesogenic side groups, adjusting the copolymer composition controls the optical birefringence of the reoriented film with effective cooperative molecular reorientation, which depends on the inherent birefringence of the aromatic acid moieties. Another purpose is to apply a reoriented film to a low-molecular LC alignment layer in order to investigate the LC alignment behavior in detail. For all the copolymer films, the LC alignment direction can be controlled both perpendicular and parallel to **E** of LPUV light, but the molecular reorientation and the type of the H-bonded mesogenic groups affect the LC alignment behavior.

2. Experimental Section

2.1. Materials. All starting materials were used as received from Tokyo Kasei Chemicals. Methacrylate monomers 6CAM and 6BAM were synthesized according to the literature,[21] and the synthetic procedure of 6PBAM and copolymer synthesis are described in the Supporting Information.

2.2. Photoreaction. Thin polymer films, which were approximately 0.2−0.3 μm thick, were prepared by spin-coating a tetrahydrofuran (THF) or *N,N*-dimethylformamide (DMF) solution of polymers (0.5−2% w/w) onto quartz or KBr substrates. The photoreactions were performed using an ultrahigh-pressure Hg lamp equipped with Glan-Taylor polarizing prisms and a cut-filter under 290 nm to obtain LPUV light with an intensity of 10 mW cm^{-2} at 365 nm. The degree of the photoreaction was estimated by monitoring the decrease in absorbance at 314 nm using UV spectroscopy for **P6CA** and BA-CA copolymer films and at 340 nm after eliminating the absorption of PBA groups for PBA-CA copolymer films.

2.3. Characterization. ^{1}H-NMR spectra using a Bruker DRX-500 FT-NMR and FTIR spectra (JASCO FTIR-410) confirmed the monomers and polymers. The molecular weight of a copolymer was measured after modifying the aromatic acid groups to the methyl ester. After esterification, the copolymers became soluble in chloroform. The molecular weight of the copolymer methyl ester was measured by GPC (Tosoh HLC-8020 GPC system with a Tosoh TSKgel column; eluent, chloroform) calibrated using polystyrene standards. A detailed procedure for the esterification of the copolymers is described in the Supporting Information. The thermal properties were examined using a polarization optical microscope (POM; Olympus BHA-P) equipped with a Linkam TH600PM heating and cooling stage in addition to differential scanning calorimetry (DSC; Seiko-I SSC5200H) analysis at a heating and cooling rate of 10 °C min^{-1}. The polarization absorption spectra were measured with a Hitachi U-3010 spectrometer equipped with Glan-Taylor polarization prisms. The temperature controlled FTIR spectra were recorded through a JASCO IRT-3000/FTIR-410 system with a Linkam TH600PM heating and cooling stage.

Table 1. Molecular Weight and Thermal Property of Synthesized (Co)Polymers

		molecular weight (g/mol)[b]			
polymer	n	x[a]	$M_n \times 10^{-4}$	M_w/M_n	thermal properties[c] (°C)
P6CA		0	3.47	2.92	G 135 N 184 I
P6(BA5-CA)	1	5	2.08	3.41	G 139 N 178 I
P6(BA25-CA)	1	25	1.80	4.01	G 136 N 178 I
P6(BA50-CA)	1	50	2.04	3.50	G 138 N 177 I
P6(BA75-CA)	1	75	1.37	4.12	G 137 N 175 I
P6(BA95-CA)	1	95	1.74	3.89	G 141 N 179 I
P6(PBA25-CA)	2	25	2.39	3.54	G 140 N 207 I
P6(PBA50-CA)	2	50	2.19	2.93	G 155 N 240 I
P6(PBA95-CA)	2	75	2.35	2.89	G 161 N 262 I
P6BA	1	100	3.50	3.52	G 157 N 179 I
P6PBA	2	100	1.34	3.92	G 188 N 299 I

[a] Determined by ^{1}H NMR. [b] Molecular weight is determined by using the methyl ester of the (co)polymer. Measured with GPC, chloroform eluent, polystyrene standards. [c] Key: G, glass; N, nematic; I, isotropic. Determined by DSC.

The photoinduced optical anisotropy, ΔA, which is expressed as eq 1, was evaluated using the polarization absorption spectra,

$$\Delta A = A_{\parallel} - A_{\perp} \tag{1}$$

where $A_{\parallel}$ and $A_{\perp}$ are the absorbances parallel and perpendicular to **E**, respectively. The thermally enhanced molecular reorientation was conducted by annealing an exposed film at an elevated temperature for 10 min. The in-plane order was evaluated using the reorientational order parameter, S, which is expressed as eq 2.[18] This equation directly means that the reorientation direction is parallel to **E** of the LPUV light for $S > 0$ and perpendicular for $S < 0$.

$$S = \frac{A_{\parallel} - A_{\perp}}{A(\text{large}) + 2A(\text{small})} \tag{2}$$

where $A_{\parallel}$ and $A_{\perp}$ are the absorbances parallel and perpendicular to **E**, respectively, and $A_{(\text{large})}$ is the larger value of $A_{\parallel}$ and $A_{\perp}$, and A(small) is the smaller one. Additionally, this equation appropriately expresses the orientation order of the mesogenic groups for both directions. The birefringence (Δn) of a reoriented film was measured by the Senarmont method at 633 nm.[44]

2.4. LC Alignment. A parallel LC cell was fabricated using two LPUV photoreacted copolymer films to evaluate the LC alignment behavior. The cell (12.5-μm thick) was filled with a nematic LC mixture (ZLI4792: Merck Japan, T_i = 102 °C) doped with 0.1 wt % of disperse blue 14 (Aldrich Co.) at 110 °C and then slowly cooled. The homogeneous LC alignment direction and the orientational order of the DB14 were evaluated from a dichroic absorption measurement utilizing the guest−host effect.

3. Results and Discussion

3.1. Synthesis and Thermal and Spectroscopic Properties of Copolymers. All copolymers were synthesized by the free radical copolymerization in THF solution. The synthesized BA-CA copolymers and **P6(BA25-CA)** were soluble in THF, but **P6(PBA50-CA)** and **P6(PBA75-CA)** precipitated during polymerization in THF but were soluble in DMF. All the synthesized copolymers exhibited a nematic LC mesophase and the LC temperature range depended on the copolymer composition as summarized in Table 1. For BA-CA copolymers, T_i in the copolymer slightly decreased when the BA composition increased because T_i of the homopolymer **P6BA** is slightly lower than that of **P6CA**. On the other hand, the LC temperature range of PBA-CA copolymer greatly depended on the copolymer

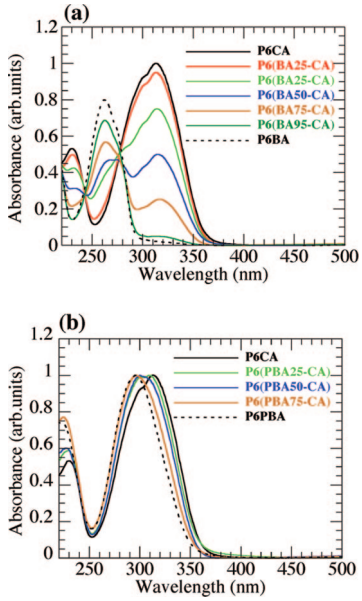

Figure 2. UV−vis absorption spectra of (a) BA-CA copolymer and (b) PBA-CA copolymer films on quartz substrates.

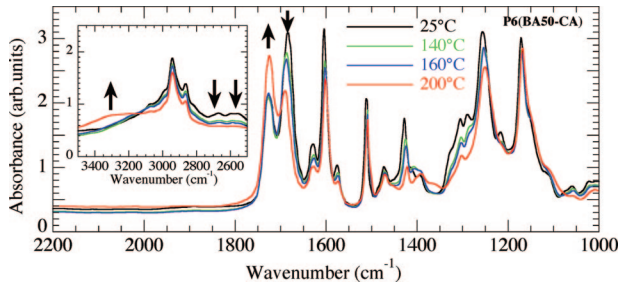

Figure 3. FT-IR spectra of the **P6(BA50-CA)** film on a KBr substrate at various temperatures.

composition and the T_i's linearly varied with the composition. Because the LC temperature range of a homopolymer with PBA groups (**P6PBA**) was much higher than that of **P6CA**, the LC temperature of PBA-CA copolymer increased as the PBA composition increased. These results indicate that the LC nature of the copolymers is attributed to randomly formed H-bonded dimers among the CA, BA, and PBA side groups.

Thin transparent copolymer films were prepared by the spin-coating method from a THF or DMF solution. Parts a and b of Figure 2 show the UV−vis absorption spectra of the copolymer films on quartz substrates. For BA-CA copolymers, absorption maxima for the BA groups (λ = 262 nm) and CA groups (λ = 314 nm) were independently observed, while the absorption band of PBA groups (λ = 295 nm) overlapped with that of the CA groups for PBA-CA copolymer films, resulting in broad absorption curves.

The formation of the H-bonding among the acid side groups was detected by the FT-IR spectrum. For example, Figure 3 shows the FT-IR spectra of a **P6(BA50-CA)** film spin-coated on a KBr substrate at various temperatures. A broad absorption around 2700 and 2550 cm^{-1}, and an absorption band at 1683 cm^{-1} were seen at room temperature, which are ascribed to H-bonded OH and C═O groups of acid side groups, respectively. These absorption bands were observed in the LC temperature range of the material. When the film was heated at 200 °C, the absorbances of H-bonded C═O and OH bands decreased, but the absorbance at 3300 cm^{-1} (free OH groups) and 1725 cm^{-1} (C═O of methacrylate and free acid groups) increased. This means that the dissociation of the H-bonds occurs in the isotropic temperature range. Additionally, when the film was cooled to room temperature, the spectrum returned to the initial one. Other copolymer films showed similar phenomena (see Supporting Information), but thermal degradation is observed when the film was heated higher than 260 °C.

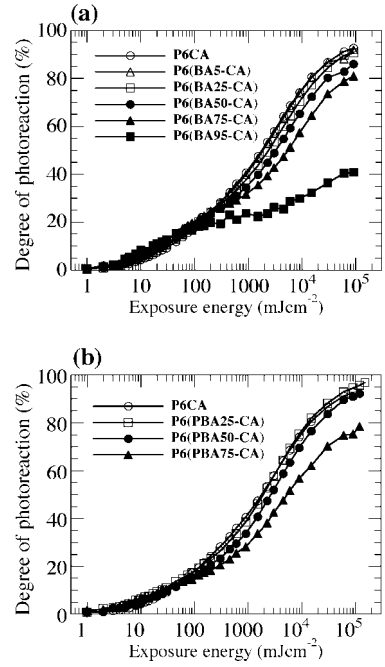

Figure 4. Degree of the photoreaction (DP) of copolymer films as a function of exposure energy. Key: (a) BA-CA copolymer films; (b) PBA-CA copolymer films.

3.2. Photoreaction of Copolymer Films with LPUV Light. Exposing a thin copolymer film to UV light leads to photoisomerization and [2 + 2] photo-cross-linking of the C═C bond of the CA groups.[21] Parts a and b of Figure 4 plot the degree of the photoreaction (DP) for the CA groups of the film as a function of exposure dose, which was estimated by measuring the decrease of the absorption intensity at 314 nm for BA-CA copolymers and at 340 nm for PBA-CA copolymers. After the photoreaction, films became insoluble in organic solvents, indicating the photo-cross-linking reaction occuered. For BA-CA copolymers, the photoreactivity in the early stage of the photoreaction did not depend on the copolymer composition, but the photoreactivity for the larger content of BA groups decreased when DP was greater than 30%, especially for **P6(BA95-CA)**, as shown in Figure 4a. This is because that the [2 + 2] photodimerization reaction becomes difficult for copolymers with a lower content of CA groups as the photoreaction proceeds. A similar tendency was observed for PBA-CA copolymers as shown in Figure 4b.

The photoreaction of the CA groups occurred axis-selectively, resulting in the negative optical anisotropy ($\Delta A < 0$) of the film.[21] Parts a and b of Figure 5 plot ΔA values as a function of exposure dose where the ΔA values are normalized at 314 nm, and are calculated by eliminating the absorption of PBA groups for the PBA-CA copolymers. These figures show that the photoinduced ΔA values are similar to each other in the early stage of the photoreaction, but they reach maxima when the degree of the photoreaction is 30−50%, and further irradiation decreases ΔA values due to the saturation of the photoreaction. These results are similar to the axis-selective photoreaction of the polymeric films comprising cinnamate groups.[11,13–16]

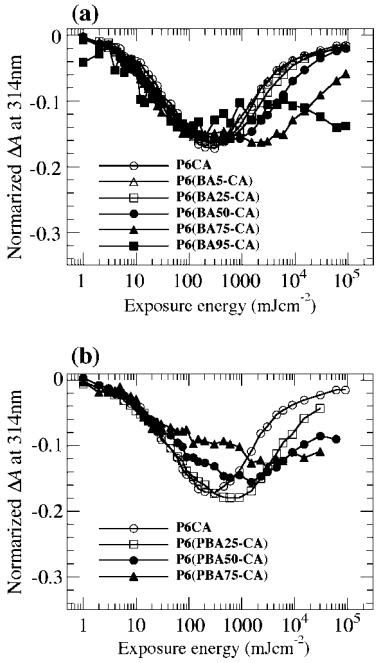

Figure 5. Normalized photoinduced optical anisotropy (ΔA) of copolymer films at 314 nm as a function of exposure energy. Initial absorbance is normalized to 1.0. Key: (a) BA-CA copolymer films; (b) PBA-CA copolymer films.

3.3. Thermal Amplification of Photoinduced Optical Anisotropy. The photoinduced small optical anisotropy of the copolymer films was thermally amplified to generate a uniaxially molecular-oriented film. Parts a and b of Figures 6 show the changes in the polarization UV−vis spectra of **P6(BA50-CA)**and **P6(BA75-CA)** films irradiated with 10 and 12 mJ cm^{-2} doses of LPUV light, respectively, and subsequent annealing at 150 °C for 10 min. In these cases, the DP was approximately 5−9 mol %. Both figures show that the annealing process enhances the negative ΔA of both the BA and CA side groups perpendicular to **E** of LPUV light, indicating thermally amplified cooperative reorientation of all the H-bonded mesogenic side groups. This is caused by the axis-selective photoreacted CA groups parallel to **E**, which reduce the LC mesomorphism in the parallel direction of the film. The subsequent annealing process generated a thermally generated self-organization perpendicular to **E** due to its stable LC mesomorphism in the perpendicular direction.[21] Thermal amplification of the photoinduced negative optical anisotropy was observed in azobenzene-containing LC polymers and PLCP films.[18,45–47] The in-plane orientational order parameter *S* values at 262 and 314 nm for the **P6(BA50-CA)** film were amplified from −0.005 to −0.67 and −0.011 to −0.68, respectively, and the birefringence (Δn) of the reoriented film was 0.128. Similar to the **P6(BA50-CA)** film, *S* values were amplified for the **P6(BA75-CA)** film. Additionally, for both cases, the sum of the absorption of $A_{\parallel}$ and $A_{\perp}$ after annealing was greater than that after exposure, suggesting that the H-bonded mesogenic side groups, including the out-of-plane direction before annealing, uniaxially reorient in the in-plane direction after the annealing procedure. The other BA-CA copolymer films show similar thermally enhanced molecular reorientation behavior as summarized in Table 2, which lists the maximum thermally enhanced in-plane *S* values of the copolymer films. It is noteworthy that the required degree of the photoreaction to obtain a large negative *S* value was higher when the BA content was larger. The required amount of the photoreacted mesogenic CA groups in the total H-bonded aromatic mesogenic groups was adjusted to be 2−5 mol % for the effective thermally enhanced molecular reorientation perpendicular to **E**.

Unlike the BA-CA copolymers, a large thermal cooperative amplification of the photoinduced ΔA for PBA-CA copolymers was observed only when the PBA content was less than 50 mol %. For the **P6(PBA50-CA)** film, the *S* value at 314 nm was amplified from −0.009 to −0.71 as shown in Figure 6c, and the generated Δn of the reoriented film was 0.178. A similar cooperative molecular reorientation behavior was observed for the **P6(PBA25-CA)** film as summarized in Table 2. However, thermal amplification rarely occurred when the PBA composition was 75 mol % as shown in Figure 6d. Because the LC temperature range of **P6(PBA75-CA)** is higher than other copolymers, H-bonding of the photoreacted CA groups will dissociate and will not generate self-organization of the copolymer film during the annealing process. Further discussion is described in section 3.4.

One of the features of copolymerization of the BA or PBA groups with **P6CA** is the controllability of the optical birefringence of the reoriented film. Figure 7 plots the thermally enhanced *S* values and the generated Δn at 633 nm for the reoriented copolymer films. For BA-CA copolymer films, the Δn value decreased when the BA composition increased, where the *S* values of the reoriented films were similar. The Δn values were verified from 0.152 to 0.095 because the inherent birefringence of the BA moiety is lower than that of the CA moiety. On the other hand, the Δn value of a PBA-CA copolymer film increased as the PBA composition increased. The largest inherent birefringence of the PBA moiety among CA, BA, and PBA groups leads to a larger Δn values for the reoriented PBA-CA copolymer films up to 0.178 (**P6(PBA50-CA)**). Thus, adjusting the copolymerization ratio controls the photoinduced birefringence of the reoriented copolymer film.

3.4. Influence of the Annealing Temperature on the Thermal Amplification of ΔA. The annealing temperature affects the efficiency of the thermal amplification of the photoinduced ΔA of the film. Parts a and b of Figure 8 plot the amplified *S* values of the BA-CA copolymer (at 314 nm) and PBA-CA copolymer (at 314 nm) films, respectively, when the exposed film is annealed at various temperatures. In these cases, the degree of the photoreaction was adjusted in order to obtain maximum negative *S* values at the appropriate annealing temperature as summarized in Table 2. Figure 8a shows that the effective amplification occurred for all the BA-CA copolymer films when the annealing temperature was between 140 and 160 °C. This temperature range is 20−40 °C lower than T_i of the copolymers. The annealing procedure close to T_i of the film was inaccessible for the effective thermal amplification of the photoinduced ΔA of the film due to the gradual dissociation of the H-bonding of the mesogenic side groups, which reduced the LC nature of the film.

In contrast, for PBA-CA copolymers the adequate annealing temperature for the effective molecular reorientation depended on the copolymer composition because the PBA unit increased the LC temperature range of the material, as shown in Figure 8b. The effective annealing temperature for **P6(PBA25-CA)** was 175−190 °C, while that for **P6(PBA50-CA)** was 180−220 °C, indicating that the annealing the exposed film in the LC temperature up to (T_i-20)°C enhances the photoinduced ΔA as with the BA-CA copolymers. However, for **P6(PBA75-CA)**, effective thermal amplification of ΔA rarely occurred regardless of temperature. This should be related to the higher content of PBA groups, but homopolymer **P6PBA** has also revealed a thermally enhanced photoinduced optical anisotropy as shown in Figure 9, which shows that the annealing the exposed **P6PBA** film at 250 °C enhanced the *S* value from −0.015 to −0.32. A similar phenomenon has also been reported in a homopolymer

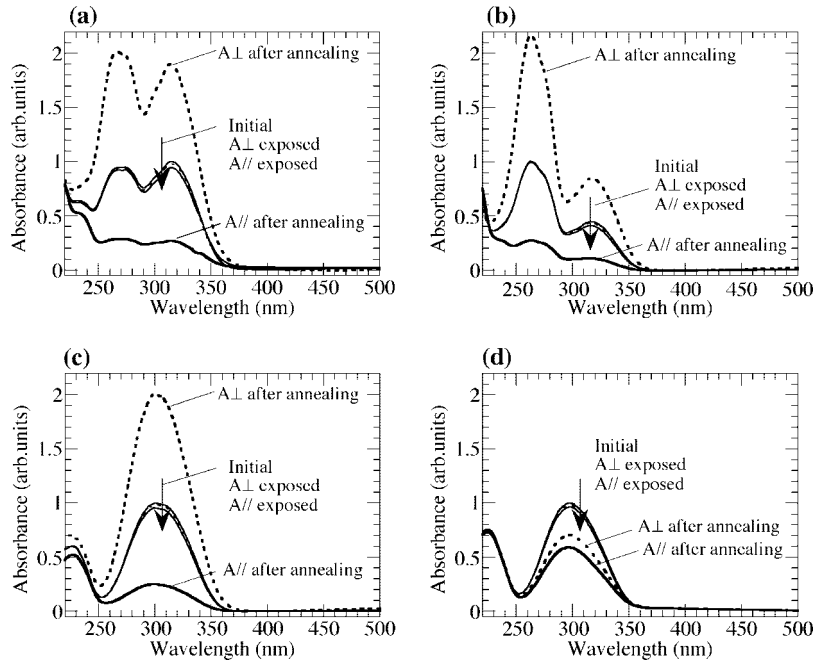

Figure 6. UV−vis polarization spectrum of copolymer films before photoirradiating, after irradiating (thin lines), and after subsequent annealing (thick lines) for 10 min. Solid line represent $A_{\parallel}$, while dotted lines show $A_{\perp}$. Key: (a) **P6(BA50-CA)**, irradiating with 10 mJ cm^{-2} doses and annealed at 150 °C; (b) **P6(BA75-CA)**, irradiating with 12 mJ cm^{-2} doses and annealed at 150 °C; (c) **P6(PBA50-CA)**, irradiating with 25 mJ cm^{-2} doses and annealed at 200 °C; (d) **P6(PBA75-CA)**, irradiating with 50 mJ cm^{-2} doses and annealed at 220 °C.

Table 2. Photoinduced and Thermally Enhanced In-Plane Order (*S*) of Copolymer Films

				S values			
				initial[b]		annealed[c]	
polymer	exposure energy (mJ/cm^2)	DP[a] (%)	annealing temp (°C)	262 nm	314 nm	262 nm	314 nm
P6CA	9	3	150		−0.009		−0.62
P6(BA5-CA)	8	3	150	−0.012	−0.011	−0.55	−0.60
P6(BA25-CA)	9	5	150	−0.003	−0.009	−0.59	−0.62
P6(BA50-CA)	10	5	150	−0.005	−0.011	−0.67	−0.68
P6(BA75-CA)	12	9	150	−0.003	−0.017	−0.71	−0.70
P6(BA95-CA)	30	14	165	−0.001	−0.031	−0.59	−0.45
P6(PBA25-CA)	10	6	180		−0.008		−0.65
P6(PBA50-CA)	25	11	200		−0.009		−0.71
P6(PBA75-CA)	50	12	220		−0.007		−0.07

[a] Degree of photoreaction of CA groups. [b] *S* values after exposing. [c] Annealed for 10 min.

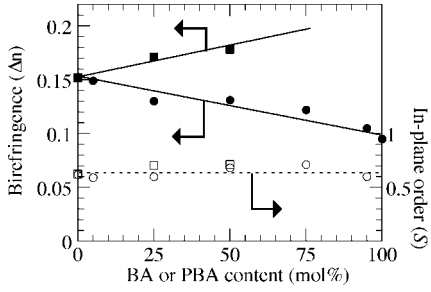

Figure 7. Thermally enhanced *S* values (open points) and birefringence (Δn) at 633 nm (closed points) when the copolymer composition is varied. Circles: BA-CA copolymer films. Squares: PBA-CA copolymers.

P6BA film where prolonged irradiation with LPUV light leads to a certain amount of axis-selective photodegradation of the BA mesogenic side groups, which then act as impurities to reduce the LC nature. Moreover, the subsequent annealing process generates molecular reorientation perpendicular to **E** as with the CA containing polymeric films.[43] Likewise in the **P6BA** film, the axis-selectively photodegraded PBA groups act as impurities to thermally generate the molecular reorientation, indicating that H-bonding of the PBA groups is not decomposed during molecular reorientation at 250 °C. Considering these results, the small amount of photoreacted CA groups and remaining H-bonded CA groups in the **P6(PBA75-CA)** film dissociated at elevated temperatures, and should not generate thermally induced self-organization.

3.5. Influence of the Exposure Doses for the Thermal Amplification of ΔA. Sections 3.3 and 3.4 described the thermal enhancement of the photoinduced ΔA perpendicular to **E** in the early stage of the photoreaction. Because irradiating with LPUV light induces photo-cross-linking of the CA groups in the copolymer film, the DP should affect the thermally amplified molecular reorientation behavior. Parts a and b of Figure 10 plot the thermally enhanced *S* values for BA-CA copolymer films at 262 and 314 nm, respectively, when the DP is varied. The annealing temperature is 150 °C for **P6(BA5-CA)**−**P6(BA75-CA)** and 160 °C for **P6(BA95-CA)**. For all the BA-CA copolymer films, cooperative molecular reorientation for both BA (at 262 nm) and CA (at 314 nm) groups was observed, and the maximum negative *S* values were obtained when the amount of the photoreacted CA groups was around 2−5 mol % in the total mesogenic BA and CA groups. Similarly, great molecular reorientation perpendicular to **E** was observed in the early stage of the photoreaction for **P6(PBA25-CA)** and **P6(PBA50-CA)** films, as plotted in Figure 10c, when the annealing temperature

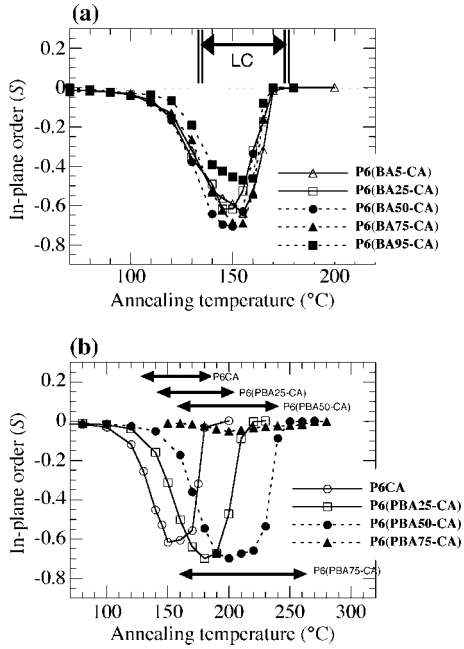

Figure 8. Thermally enhanced *S* values of the photoreacted copolymer films when the annealing temperature is varied. (a) BA-CA copolymer films and (b) PBA-CA copolymer films. Arrows exhibit the LC temperature range of materials. Degrees of the photoreaction are as follows: **P6(BA5-CA)** (3 mol %), **P6(BA25-CA)** (5 mol %), **P6(BA50-CA)** (7 mol %), **P6(BA75-CA)** (9 mol %), **P6(BA95-CA)** (14 mol %), **P6(PBA25-CA)** (6 mol %), **P6(PBA50-CA)** (10 mol %), **P6(PBA75-CA)** (12 mol %), and **P6CA** (3 mol %).

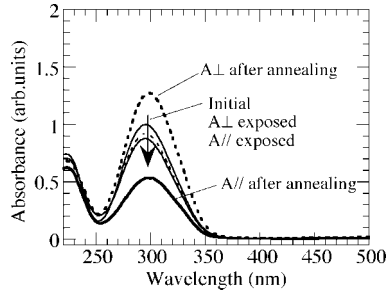

Figure 9. UV−vis polarization spectrum of a **P6PBA** film before photoirradiating, after irradiating (thin lines) with 75 Jcm^{-2} doses, and after subsequent annealing (thick lines) at 250 °C for 10 min. Solid lines represent $A_{\parallel}$, while dotted lines show $A_{\perp}$.

was 180 °C for **P6(PBA25-CA)**, and 200 °C for **P6(PBA50-CA)**, respectively. However, the photoinduced ΔA of the **P6(PBA75-CA)** film (annealing temperature of 220 °C) was rarely amplified regardless of the DP.

In contrast, a reverse amplification ($S > 0$) of the photoinduced optical anisotropy was observed for the **P6CA** and **P6(BA5-CA)** films when the DP was around 10−14 mol %, and the in-plane orientational order parameter, *S*, at 314 nm was reversely enhanced to +0.10 to +0.14. This molecular reorientation parallel to **E** was caused by the large amount of photo-cross-linked CA side-groups fixed in parallel to **E**, which acted as the photo-cross-linked anchors to thermally reorient other mesogenic groups along them.[17,18,21] However, when the copolymer includes greater than 25 mol % of BA groups (**P6(BA25-CA)** - **P6(BA95-CA)**), the thermally enhanced *S* values are close to zero when the DP is greater than 12−20 mol %, as plotted in Figure 10, parts a and b. In these cases, the photo-cross-linked H-bonded CA-BA groups cannot effectively induce the thermally enhanced self-organization of

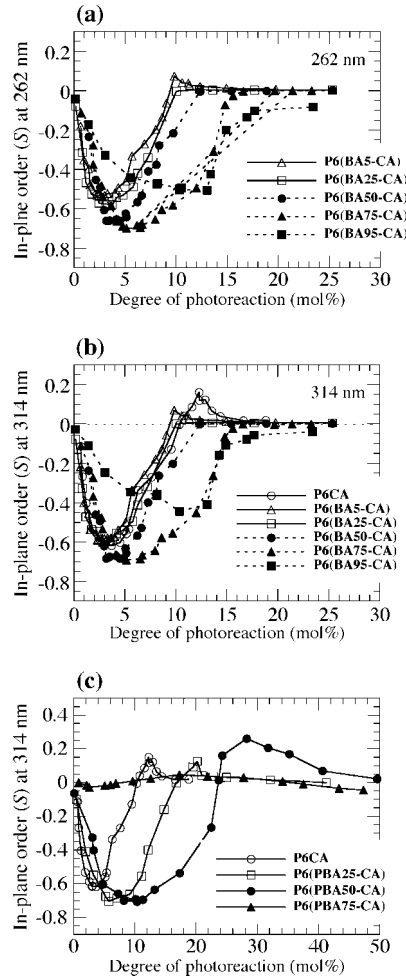

Figure 10. Thermally enhanced *S* values of the photoreacted copolymer films as a function of the degree of the photoreaction. Key: (a) BA-CA copolymer films at 262 nm, (b) BA-CA copolymer films at 314 nm, and (c) PBA-CA copolymer films at 314 nm. Annealing temperature is 150 °C for **P6CA** and **P6(BA5-CA)**- **P6(BA75-CA)**, 165 °C for **P6(BA95-CA)**, 180 °C for **P6(PBA25-CA)**, 200 °C for **P6(PBA50-CA)**, and 220 °C for **P6(PBA75-CA)**.

H-bonded BA with mesogenic groups parallel to **E**. This is due to the poor stabilization of LC characteristics of BA groups.

On the other hand, **P6(PBA25-CA)** and **P6(PBA50-CA)** films revealed molecular reorientation parallel to **E** when the DP was around 19 mol % for **P6(PBA25-CA)**, and 28 mol % for **P6(PBA50-CA)**, as plotted in Figure 10c. In these cases, the DP in the total amount of aromatic acid side groups was approximately 13−18 mol %. The *S* values at 314 nm were reversely enhanced from −0.035 to +0.13 for **P6(PBA25-CA)**, and from −0.036 to +0.29 for **P6(PBA50-CA)**, respectively. However, regardless of the DP, **P6(PBA75-CA)** did not show an effective molecular reorientation, which is due to the thermal dissociation of the H-bonded CA groups as described in 3.4. Because the LC mesomorphism of the H-bonded PBA mesogenic groups is more stable than that of BA groups due to the biphenyl moiety in PBA, the photo-cross-linked CA-PBA groups in **P6(PBA25-CA)** and **P6(PBA50-CA)** act as effective photo-cross-linked anchors to thermally reorient the H-bonded mesogenic side groups for both the PBA and CA groups. These results suggest that the liquid crystallinity of the H-bonded mesogenic groups plays an important role in the thermally enhanced reorientation parallel to **E**, which is generated by the photo-cross-linked anchors. Namely, the order of strength for the thermally enhanced molecular reorientation parallel to **E** is

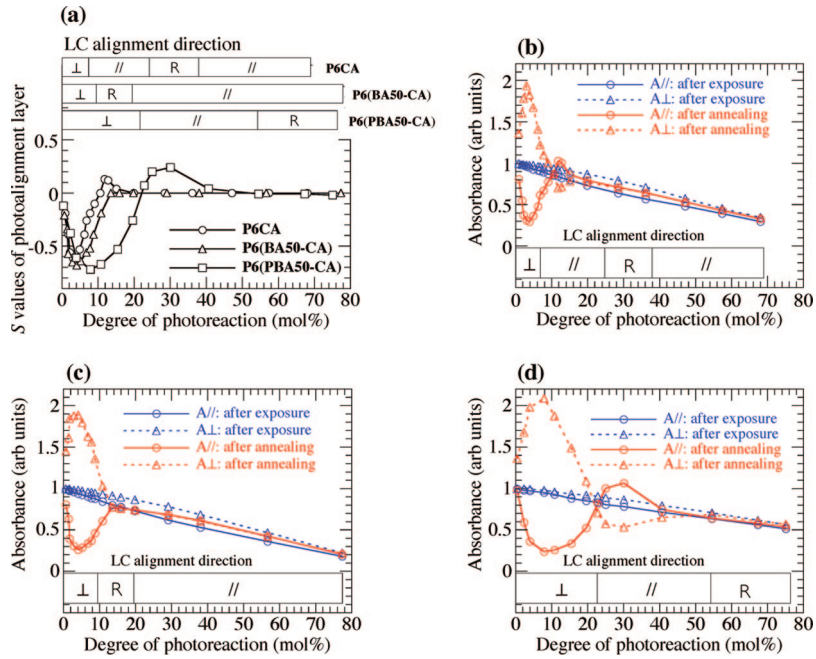

Figure 11. (a) Order parameter (*S*) of the photoalignment layer of **P6CA**, **P6(BA50-CA)** and **P6(PBA50-CA)** films, and the LC alignment direction in the LC cell using two corresponding photoalignment films as a function of DP of the photoalignment film. (b−d) Change in the absorbance at 314 nm of (b) **P6CA**, (c) **P6(BA50-CA)**, and (d) **P6(PBA50-CA)** films after exposure and after subsequent annealing, and the LC alignment direction as a function of DP. LC alignment direction: ⊥ is perpendicular to **E**, || is parallel to **E**, and R is random orientation.

photo-cross-linked H-bonded PBA-CA, CA-CA, and BA-CA mesogenic groups.

3.6. LC Alignment. We previously reported that a reoriented **P6CA** film is applicable to the alignment layer for low-molecular LCs.[21] Reoriented copolymer films also show homogeneous LC alignment ability. Figure 11a plots the *S* values of the reoriented **P6CA**, **P6(BA50-CA)** and **P6(PBA50-CA)** films, and the LC alignment direction using two corresponding photoalignment films as a function of the DP. When LC molecules aligned homogeneously, the order parameter of the dichroic dye (DB14) at 653 nm was around 0.4 in all cases, and disclinations were not observed in the LC cell.

The LCs aligned perpendicular to **E** on the **P6CA** film, when the DP was between 0.5−6.5 mol %. LC alignment perpendicular to **E** was also observed for both **P6(BA50-CA)** and **P6(PBA50-CA)** films when the DP was between 0.4−9.0 mol % for **P6(BA50-CA)** and 0.5−21 mol % for **P6(PBA50-CA)**. In these cases, H-bonded mesogenic groups of the (co)polymer films effectively reoriented perpendicular to **E**. The interaction between the LC molecules and the H-bonded mesogenic groups in the (co)polymer film reoriented perpendicular to **E** induced the LC alignment perpendicular to **E**, where the LC molecules aligned along the reoriented H-bonded mesogenic groups in the photoalignment layer.

As the DP proceeded, the alignment direction changed to parallel to **E**. Several types of photoalignment layers can control the LC alignment direction by adjusting the exposure doses.[3,16,48,49] For the **P6CA** film, parallel LC alignment was observed when the DP was between 6.8−9.0 mol %, although the reorientation direction of the photoalignment layer remained perpendicular to **E**. This observation is attributed to the larger azimuthal anchoring of the photoreacted H-bonded CA-CA groups parallel to **E** rather than the partially reoriented H-bonded CA mesogenic groups perpendicular to **E**.[21] The higher DP of the film revealed a parallel LC alignment where the reorientation direction of the photoalignment layer was parallel to **E** (the DP is between 10−21 mol %), which is due to the strong interaction between the LC molecules as well as the photoreacted (mainly the photo-cross-linked) and reoriented H-bonded CA-CA groups parallel to **E**. However, LCs once randomly aligned when the DP was approximately 28−37 mol %, were aligned parallel to **E** again upon further increasing the DP. In these DP ranges, the reorientational order of the alignment film was close to zero, but $A_{||}$ of the photoalignment film slightly increased after annealing, while $A_{\perp}$ decreased when observing the change in the absorbance of the photoalignment film in detail as plotted in Figure 11b. This means that the annealing procedure partially generates molecular reorientation parallel to **E** of the **P6CA** film. The large amount of the photo-cross-linked H-bonded CA-CA groups and the small amount of molecular reorientation parallel to **E** caused parallel LC alignment, but random LC alignment also appeared when azimuthal anchoring between the parallel and perpendicular direction of the photoalignment layer is rivaled. Because the LC alignment is caused by the interaction between the LC molecules and the surface of the photoalignment layer, the amount of photoreacted H-bonded CA-CA groups and the state of molecular orientation of the polymer surface touching the LC molecules must be evaluated to elucidate this unique LC alignment behavior.

In contrast, LCs exhibited a random orientation for the **P6(BA50-CA)** film when DP was between 10−17 mol %, and the reorientational order of the alignment film was between −0.19 and 0 as plotted in Figure 11, parts a and c. Unlike **P6CA**, the interaction between the LC molecules and the photoreacted H-bonded CA-BA groups was comparable to that between LCs and the reoriented other mesogenic groups at this DP range. Namely, the azimuthal anchoring energy of thephotoreacted H-bonded CA-BA groups is smaller than that of the photoreacted H-bonded CA-CA groups. A small anchoring energy of the photoreacted H-bonded CA-BA groups is related to the fact that the CA-BA copolymer films do not exhibit an effective molecular reorientation parallel to **E** as described in section 3.5. Interestingly, a parallel LC alignment was observed when the DP was greater than 20 mol %, but the orientational order of the copolymer film was close to zero. In this DP range, $A_{||}$ of the photoalignment film slightly increased after annealing, while

$A_\perp$ decreased as plotted in Figure 11c, due to the partial reorientation of the H-bonded CA-BA mesogenic groups which is caused by the large amount of the photo-cross-linked H-bonded CA-BA groups parallel to **E** and results in the parallel LC alignment similar to the **P6CA** film with a higher DP range.

For the **P6(PBA50-CA)** film, the LC alignment direction was consistent with the reorientational direction of the photoalignment film, as plotted in Figure 11, parts a and d, implying that the LC alignment direction is controlled by the reorientation direction of the H-bonded PBA and CA groups when the interaction between the LC molecules and the biphenyl groups in the H-bonded PBA moiety is larger than that of CA or BA groups due to the stable LC mesomorphism of **P6(PBA50-CA)**. Additionally, a uniform LC alignment was not observed when the DP was greater than 55 mol %, and the molecular reorientation barely occurred as plotted in Figure 11d. The molecular motion of the PBA moiety cannot occur at elevated temperatures when the film exhibits a higher degree of the photo-cross-linked structure. Thus, the LC alignment direction is controlled for the molecular reorientation and the molecular structure of the photoalignment film, and these matters will influence the anchoring energy of the photoalignment layer. A quantitative investigation of the azimuthal anchoring energy of the photoalignment (co)polymer films is in progress.

4. Conclusion

Polymethacrylate liquid crystalline copolymers, which have a hexamethylene spacer group terminated with CA, BA, or PBA in the side chain were synthesized and characterized. All the synthesized copolymers exhibited nematic LC mesomorphism due to H-bonding among the aromatic acid side groups. Irradiating a thin film with LPUV light generated a small photoinduced optical anisotropy based on the axis-selective photoreaction of the H-bonded dimers containing the CA moiety. Subsequent annealing in the LC temperature range of the copolymer films induced a cooperative molecular reorientation for all the H-bonded mesogenic groups perpendicular to **E** of LPUV light where the required exposure energy was 8−30 mJ cm^{-2} with an orientational order of greater than 0.6. Adjusting the copolymer composition controlled the generated birefringence from 0.095 to 0.152 for BA-CA copolymers, and from 0.152 to 0.178 for PBA-CA copolymers. Additionally, molecular reorientation parallel to **E** was also achieved for CA homopolymer and CA-PBA copolymer films, while BA-CA copolymer films with BA composition greater than 25 mol % did not show parallel reorientation. The difference in the photoreacted products and the liquid crystalline characteristcs among the H-bonded CA, BA, and PBA groups played an important role in the thermally enhanced reorientation parallel to **E**. Furthermore, controlling the uniaxial alignment direction of low-molecular LC on oriented copolymer films was achieved. It was clarified that the molecular reoriented structure of the (co)polymer film determined the LC alignment direction, while the interaction between the low-molecular LC and the photoreacted H-bonded mesogenic groups as well as the molecular reoriented structure influenced the LC alignment direction parallel to **E**. We anticipate that the reoriented (co)polymer films will be useful not only for birefringent films in LCDs, but also for the photoalignment layers in uniaxial and patterned LC orientations.

Acknowledgment. This work was partly supported by Grant-in-Aid for Scientific Research (S, No.16105004) by Japan Society for the Promotion of Science, and Hayashi Telempu Co., Ltd.

Supporting Information Available: Text and schemes giving the synthetic procedure of monomers and copolymers and esterification of copolymers and a figure showing the FT-IR spectrum of **P6(PBA50-CA)**. This material is free of charge via the Internet at http://pubs.acs.org.

References and Notes

(1) (a) Shibaev, V. P.; Kostromin, S. G.; Ivanov, S. A. *Polymers as Electroactive and Photooptical Media*; Shibaev, V. P., Ed.; Springer: Berlin, 1996; pp 37−110. (b) MacArdle, C. B. *Applied Photochromic Polymer Systems*; MacArdle, C. B., Ed.; Blackie: New York, 1991; pp 1−30. (c) Krongauz, V. *Applied Photochromic Polymer Systems*; MacArdle, C. B., Ed.; Blackie: New York, 1991; pp 121−173.
(2) (a) Ichimura, K. *Chem. Rev.* **2000**, *100*, 1847–1873. (b) Natansohn, A.; Rochon, P. *Chem. Rev.* **2002**, *102*, 4139–4176. (c) Ikeda, T. *J. Mater. Chem.* **2003**, *13*, 2037–2057.
(3) O'Neill, M.; Kelly, S. M. *J. Phys. D: Appl. Phys.* **2000**, *33*, R67–R84.
(4) (a) Anderle, K.; Birenheide, R.; Eich, M.; Wendrorff, J. H. *Makromol. Chem. Rapid. Commun.* **1989**, *10*, 477–483. (b) Shi, Y.; Steier, W. H.; Yu, L.; Chen, M.; Dalton, L. R. *Appl. Phys. Lett.* **1991**, *59*, 2935–2937.
(5) Kawatsuki, N.; Ono, H. *Organic Electronics and Photonics*; Nalwa, H. S., Ed.; American Sci. Publishers: Stevenson Ranch, CA, 2007; *Vol. 2*; pp 301−344.
(6) Wu, Y.; Natansohn, A.; Rochon, P. *Macromolecules* **2004**, *37*, 6801–6805.
(7) Beyer, P.; Krueger, M.; Giesselmann, F.; Zentel, R. *Adv. Funct. Mater.* **2007**, *17*, 109–114.
(8) Häckel, M.; Kador, L.; Kropp, D.; Schmidt, H.-W. *Adv. Mater.* **2007**, *19*, 227–231.
(9) Sapich, B.; Vix, A. B. E.; Rabe, J.; Stumpe, J. *Macromolecules* **2005**, *38*, 10480–10486.
(10) (a) Saishoji, A.; Sato, D.; Shishido, A.; Ikeda, T. *Langmur* **2007**, *23*, 320–326. (b) Ishiguro, M.; Sato, D.; Shishido, A.; Ikeda, T. *Langmur* **2007**, *23*, 332–338.
(11) Barachevsky, V. A. *Proc. SPIE* **1991**, *1559*, 184–193.
(12) Schadt, M.; Seiberle, H.; Schuster, A. *Nature* **1994**, *381*, 212–215.
(13) Schadt, M.; Schmitt, K.; Kozinkov, V.; Chigrinov, V. *Jpn. J. Appl. Phys.* **1992**, *31*, 2155–2164.
(14) (a) Akita, Y.; Akiyama, H.; Kudo, K.; Hayashi, Y.; Ichimura, K. *J. Photopolym. Sci. Technol.* **1995**, *8*, 75–78. (b) Ichimura, K.; Akita, Y.; Akiyama, H.; Kudo, K.; Hayashi, Y. *Macromolecules* **1997**, *30*, 903–911. (c) Obi, M.; Morino, S.; Ichimura, K. *Jpn. J. Appl. Phys.* **1999**, *38*, L145–L147.
(15) Iimura, Y.; Saitoh, T.; Kobayashi, S.; Hashimoto, T. *J. Photopolym. Sci. Technol.* **1995**, *8*, 257–262.
(16) (a) Kawatsuki, N.; Ono, H.; Takatsuka, H.; Yamamoto, T.; Sangen, O. *Macromolecules* **1997**, *30*, 6680–6682. (b) Kawatsuki, N.; Matsuyoshi, K.; Hayashi, M.; Takatsuka, H.; Yamamoto, T. *Chem. Mater.* **2000**, *12*, 1549–1555.
(17) (a) Kawatsuki, N.; Takatsuka, H.; Yamamoto, T.; Sangen, O. *J. Polym. Sci., Part A: Polym. Chem.* **1998**, *36*, 1521–1526. (b) Kawatsuki, N.; Suehiro, C.; Yamamoto, T. *Macromolecules* **1998**, *31*, 5984–5990.
(18) Kawatsuki, N.; Goto, K.; Kawakami, T.; Yamamoto, T. *Macromolecules* **2002**, *35*, 706–713.
(19) Kawatsuki, N.; Tsutsumi, R.; Takatsuka, H.; Sakai, T. *Macromolecules* **2007**, *40*, 6355–6360.
(20) (a) Kawatsuki, N.; An, M. X.; Matsuura, Y.; Sakai, T.; Takatsuka, T. *Liq. Cryst.* **2004**, *31*, 55–60. (b) Kawatsuki, N.; Tachibana, T.; An, M. X.; Kato, K. *Macromolecules* **2005**, *38*, 3903–3908. (c) Kawatsuki, N.; Kato, K.; Shiraku, T.; Ono, H. *Macromolecules* **2006**, *39*, 3245–3251.
(21) Uchida, E.; Kawatsuki, N. *Macromolecules* **2006**, *39*, 9357–9364.
(22) (a) Kawatsuki, N.; Kawakami, T.; Yamamoto, T. *Adv. Mater.* **2001**, *13*, 1337–1339. (b) Kawatsuki, N.; Sakai, T.; An, M. X.; Hasegawa, T.; Yamamoto, T. *Proc. SPIE* **2001**, *4463*, 109–116. (c) Kawatsuki, N.; An, M. X.; Hasegawa, T.; Yamamoto, T.; Sakai, T. *Jpn. J. Appl. Phys.* **2002**, *41*, L198−L200.
(23) Kawatsuki, N.; Hamano, K.; Ono, H.; Sasaki, T.; Goto, K. *Jpn. J. Appl. Phys.* **2007**, *46*, 339–341.
(24) Kawatsuki, N.; Hasegawa, T.; Ono, H.; Tamoto, T. *Adv. Mater.* **2003**, *15*, 991–994.
(25) Gray, G. W.; Jones, B. *J. Chem. Soc.* **1953**, 4179–4180.
(26) Kato, T.; Fréchet, J. M. J. *Macromolecules* **1989**, *22*, 3818–3819.
(27) (a) Kato, T.; Fréchet, J. M. J. *J. Am. Chem. Soc.* **1989**, *111*, 8533–8534. (b) Kumar, U.; Kato, T.; Fréchet, J. M. J. *J. Am. Chem. Soc.* **1992**, *114*, 6630–6639. (c) Kato, T.; Kihara, H.; Uryu, T.; Fujishima, A.; Frechet, J. M. J. *Macromolecules* **1992**, *25*, 6836–6841. (d) Kato, T.; Fukumasa, M.; Fréchet, J. M. J. *Chem. Mater.* **1995**, *7*, 368–372. (e) Kato, T.; Mizoshita, N.; Kanie, K. *Macromol. Rapid Commun.* **2001**, *22*, 797–814.
(28) Shandryuk, G. A.; Kuotsov, S. A.; Shatalova, A. M.; Plate, N. A.; Talroze, R. V. *Macromolecules* **2003**, *36*, 3417–3423.

(29) (a) Lin, H.-C.; Sheu, H.-Y.; Chang, C.-L.; Tsai, C.-M. *J. Mater. Chem.* **2001**, *11*, 2958–2965. (b) Lin, H.-C.; Tsai, C.-M.; Huang, G.-H.; Tao, Y.-T. *Macromolecules* **2006**, *39*, 557–568.
(30) Lin, H.-C.; Hendrianto, J. *Polymer* **2005**, 12146–12157.
(31) (a) Fischer, Th.; Läsker, L.; Stumpe, J.; Kostromin, S. G. *J. Photochem. Photobiol. A: Chem.* **1994**, *80*, 453–459. (b) Läsker, L.; Fischer, Th.; Stumpe, J.; Kostromin, S. G.; Ivanov, S.; Shivaev, V.; Ruhmann, R. *Mol. Cryst. Liq. Cryst.* **1994**, *246*, 347–350.
(32) Buffeteau, T.; Natansohn, A.; Rochon, P.; Pézolet, M. *Macromolecules* **1996**, *29*, 8783–8790.
(33) (a) Wu, Y.; Demachi, Y.; Tsutsumi, O.; Kanazawa, A.; Shiono, T.; Ikeda, T. *Macromolecules* **1998**, *31*, 349–354. (b) Wu, Y.; Demachi, Y.; Tsutsumi, O.; Kanazawa, A.; Shiono, T.; Ikeda, T. *Macromolecules* **1998**, *31*, 1104–1108.
(34) Natansohn, A.; Rochon, P.; Meng, X.; Barrett, C.; Buffeteau, T.; Bonenfant, S.; Pézolet, M. *Macromolecules* **1998**, *31*, 1155–1161.
(35) Bobrovsky, A.; Boiko, N.; Shibaev, V.; Stumpe, J. *J. Photochem. Photobiol. A: Chem.* **2004**, *163*, 347–358.
(36) Kawatsuki, N.; Matsuyoshi, K.; Yamamoto, T. *Macromolecules* **2000**, *33*, 1698–1702.
(37) Rosenhauer, R.; Stumpe, J.; Giménez, R.; Piñol, M.; Serrano, J. L.; Viñuales, A. *Macromol. Rapid Commun.* **2007**, *28*, 932–936.
(38) (a) Rosenhauer, R.; Fischer, Th.; Stumpe, J.; Giménez, R.; Piñol, M.; Serrano, J. L.; Viñuales, A.; Boer, D. *Macromolecules* **2005**, *38*, 2213–2222. (b) Giménez, R.; Millaruelo, M.; Piñol, M.; Serrano, J. L.; Viñuales, L.; Rosenhauer, R.; Stumpe, J. *Polymer* **2005**, *46*, 9230–9242.
(39) Lin, H.-C.; Tsai, C.-M.; Huang, G.-H.; Tao, Y.-T. *Macromolecules* **2006**, *30*, 557–568.
(40) Gao, J.; He, Y.; Liu, F.; Zhang, X.; Wang, Z.; Wang, X. *Chem. Mater.* **2007**, *19*, 3877–3881.
(41) Medvedev, A. V.; Barmatov, E. B.; Medvedev, A. S.; Shibaev, V. P.; Ivanov, S. A.; Kozlovsky, M.; Stumpe, J. *Macromolecules* **2005**, *38*, 2223–2229.
(42) Osuji, C. O.; Chao, C.-Y.; Ober, C. K.; Thomas, E. L. *Adv. Funct. Mater.* **2002**, *12*, 753–758.
(43) Kawatsuki, N.; Uchida, E. *Polymer* **2007**, *48*, 3066–3073.
(44) El-Hosseiny, F. *J. Opt. Soc. Am.* **1975**, *65*, 1279–1282.
(45) (a) Han. M.; Ichimura, K. *Macromolecles* **2001**, *34*, 90–98. (b) Han, M.; Morino, S.; Ichimura, K. *Macromolecles* **2000**, *33*, 6360–6370. (c) Kidowaki, M.; Fujiwara, T.; Ichimura, K. *Chem. Lett.* **1999**, *28*, 641–642.
(46) Wu, Y.; Zhang, Q.; Kanazawa, A.; Shiono, T.; Ikeda, T.; Nagase, Y. *Macromolecules* **1999**, *32*, 3951–3956.
(47) Uchida, E.; Shiraku, T.; Ono, H.; Kawatsuki, N. *Macromolecules* **2004**, *37*, 5282–5291.
(48) Jackson, P. O.; O'Neill, M.; Duffy, W. L.; Hindmarsh, P.; Kelly, S. M.; Owen, G. J. *Chem. Mater.* **2001**, *13*, 694–703.
(49) Trajakovska, A.; Kim, C.; Marshall, K. L.; Mourey, T.; Chen, S. H. *Macromolecules* **2006**, *39*, 6983–6989.

MA800505C